

# NUMERICAL ANALYSIS OF THERMAL AND FLOW CHARACTERISTICS IN LOUVERED FIN HEAT EXCHANGERS WITH NOVEL FIN DESIGNS

*Nandhakumar SHANKAR<sup>1\*</sup>, Satheesh Kumar SANKARA NARAYANA RAMA VIJAYAM<sup>2</sup>,  
Keerthivasan KUNJUPILLAI CHANDRASEKARAN<sup>3</sup>, Raju KANDASAMY<sup>4</sup>*

<sup>\*1,3,4</sup>Department of Mechanical Engineering, M.Kumarasamy College of Engineering, Karur, Tamil Nadu-639113, India.

<sup>2</sup>Department of Mechanical Engineering, SRM Institute of Science and Technology – Ramapuram Campus, Chennai-600089, Tamilnadu, India.

\* Corresponding author; E-mail: snks.nandhakumar@gmail.com

*This study presents the design and performance evaluation of novel louver fin geometries aimed at improving the air-side thermo-hydraulic performance of compact heat exchangers. While prior research has primarily explored traditional fin configurations, a significant gap remains in systematically analysing the impact of unconventional fin shapes and geometry dimension modifications. To address this, several innovative fin geometries were developed and assessed using computational fluid dynamics (CFD) under turbulent flow conditions. The performance metrics were evaluated across a Reynolds number range of 125–945, with a focus on the Colburn j-factor and friction factor (f-factor) to quantify heat transfer enhancement and pressure drop. While higher Reynolds numbers improved heat transfer and Nusselt number, gains tapered off at extreme flow rates. It was observed that optimized geometric configurations (the 120° louver angle with 20% pitch) led to a significant enhancement in heat transfer characteristics (high h, Nu, and j) while maintaining a relatively low pressure drop and friction factor ( $\Delta P$  and f). These trends clearly indicate a favourable thermal-hydraulic performance. The study is offering an effective approach for optimizing heat exchanger efficiency in air-cooled applications.*

*Keywords: Louver Fin Geometry, CFD Simulation, Heat Transfer Enhancement, Novel Fin Design, Compact Heat Exchanger.*

## 1 Introduction

Louvered finned heat exchangers have undergone substantial evolution, becoming crucial components in thermal systems due to their ability to enhance heat transfer while maintaining compactness. Research has progressed from basic theoretical modelling and CFD validation to detailed studies optimizing fin geometry, aspect ratios, and flow characteristics. Key developments include integrating vortex generators, turbulators, and advanced materials to improve thermal efficiency with minimal pressure loss.

More recent work explores hybrid designs, AI-based optimizations, and energy system applications like PV/T collectors, radiators, and solar heaters. Kays and London's (1984) [1] Compact Heat Exchangers provides the foundational correlations and performance maps for various fin geometries, including louvered and plate fins, establishing the widely used relationships for air-side heat transfer and pressure-drop prediction. Their systematic classification of compact heat exchanger surfaces and experimental datasets forms the basis for evaluating thermo-hydraulic performance, making it a primary reference for validating and comparing new fin designs. Shah and Sekulic (2003) [2] provide a comprehensive theoretical and practical foundation for heat exchanger design, emphasizing fundamental transport processes, flow arrangements, and performance evaluation methods. Their work also presents detailed correlations for heat transfer and pressure drop in various exchanger geometries, serving as a key reference for analysing and optimizing compact heat exchanger configurations. Shah (2020) [3] provides an in-depth overview of air-side heat transfer mechanisms, geometric effects, and flow behaviour associated with louvered fin configurations in compact heat exchangers. It also compiles advanced modelling, optimization strategies, and application-specific design considerations, offering a foundational reference for improving thermo-hydraulic performance in modern heat exchanger systems.

Subhash Chand and Prabha Chand (2018) [4] developed a theoretical model to study solar air heaters with louvered fins. Results showed thermal efficiency increased from 43.14% to 76.79%, but high mass flow rates caused a 9.4% drop in effective efficiency due to pressure loss. Rezaia et al. (2017) [5] studied on CFD study on corrugated louvered fins showed that the j-factor deviation was under 10.7%, confirming thermal accuracy, while the f-factor had larger deviations (-45.5% to 86.4%), indicating lower pressure validation certainty. Lin and Jang (2005) [3] studied EHD-enhanced plate-fin and tube heat exchangers, finding that staggered tube pitch with square electrodes improved heat transfer by 218% at  $Re = 100$  and  $VE = 16$  kV, reducing fin area by 56%.

Moosavi et al. (2021) [7] investigated how louvered fin geometry affects flow, pressure drop, and heat transfer in compact heat exchangers. A symmetrical fin layout with aligned louvers showed optimal performance, and a correlation was developed for flow deviation based on louver angle. Kim (2021) [8] found that in louver-finned aluminium heat exchangers, pressure drop increased with inclination, with minimum heat transfer at  $45^\circ$ . The new design showed better wet condition performance due to effective condensate drainage. Kannadhasan et al. (2024) [9] examined engine fins with varied geometries using experiments and CFD analysis. Aluminium alloy showed superior heat dissipation, while magnesium performed moderately, and grey cast iron had the lowest thermal efficiency. Achaichia and Cowell (1988) [10] conducted one of the earliest comprehensive studies on flat-tube and louvered plate-fin surfaces, examining their air-side heat transfer and pressure drop characteristics across a wide range of operating conditions. Their results established key correlations for the Colburn j-factor and friction factor, and importantly identified that flow transitions from laminar to turbulent when the Reynolds number based on louver pitch approaches 1300, a criterion widely adopted in subsequent louver-fin research.

Kim and Bullard (2002) [11] investigated experimentally on multi-louvered fin and flat-tube heat exchangers for analysing the air-side heat transfer and pressure drop characteristics over a Reynolds number range of 100–600 by varying louver angle, fin pitch, and flow depth. These studies reported performance

in terms of Colburn j-factor and Fanning friction factor, establishing general correlations and highlighting flow depth as a key parameter governing pressure drop. Wongwises and Chokeman (2004) [12] found that increasing fin thickness enhances heat transfer in 2-row exchangers but has mixed effects in 4 rows, depending on Reynolds number. Friction factor increases with thickness for fin pitch  $\leq 1.81$  mm but remains unchanged at 2.54 mm. Yong et al. (2024) [13] found that hexagonal twisted pin fins in rectangular channels enhance heat transfer by up to 132.71% at  $Re = 22,800$ . Performance depends on Reynolds number and fin arrangement. Zhu et al. (2023) [14] numerically showed that annular fins reduce melting time by over 10% compared to longitudinal fins in latent heat storage units. The best performance was observed in vertical units with annular fins and bottom HTF inlet. Mozafarie et al. (2019) [15] numerically analysed non-Newtonian fluid flow in a helically finned double-pipe heat exchanger. Heat transfer increased by up to 39%, with pressure drop rising up to 3 times as fin pitch decreased. Lindqvist et al. (2021) [16] studied a CFD model for plate fin-and-tube heat exchangers, showing that reducing tube pitch improved efficiency. Their results matched experimental data within 20% for most cases.

Mercan et al. (2022) [17] experimentally evaluated heavy-duty radiators with double-U grooved pipes with louvered fins, showing highest heat transfer; ANN predictions matched experimental data well. Santosa et al. (2019) [18] studied CO<sub>2</sub> gas coolers using experiments and CFD, achieving a 9% max error. Optimizing the circuit improved performance by 20%, while a slit between tube rows increased heat transfer by 8%. Li et al (2023) [19] examined a flap fin louver windcatcher that maintains steady ventilation and supports passive energy use. Tests and CFD validation proved its effectiveness, with future studies focusing on design improvements and energy recovery. Arunkmar et al. (2024) [20] analysed how the aspect ratio of louvered finned solar air heaters affects efficiency. A 4:1 ratio maximizes thermal performance, but higher mass flow rates reduce exergy efficiency due to friction losses. Kumar et al. (2024) [21] optimized louver fin geometries of a microchannel condenser using Taguchi and CFD, identifying fin pitch as the key factor. The optimal design improved Colburn-j by 24.42% and JF factor by 18.23% over the default. Malapure et al. [22] conducted a numerical study on 15 different compact louvered fin heat exchangers to analyze heat transfer and pressure drop. They found that at low Reynolds numbers, airflow follows the fin direction, while at higher Reynolds numbers, it aligns with the louver angle. Additionally, the highest Nusselt numbers were observed at the fin tip and the leading and trailing edges of the louvers. Erbay et al (2016) [23] studied numerically on louvered-fin and flat-tube heat exchangers for household refrigeration and it is shown that low-Reynolds-number air-side performance is strongly influenced by louver angle and fin pitch. The findings indicate that heat transfer and flow parameters such as the Colburn j-factor, friction factor, Stanton number, and volume goodness factor vary nonlinearly with geometric modifications, with optimal performance occurring at smaller louver angles and tighter fin spacing.

Getie et al. (2024) [24] numerically investigated louver edge effects in LFCHE, finding that horizontal edges reduced pressure drop by 24.2% and increased outlet air temperature by 1.01%, improving performance. Ali et al. (2024) [25] analysed FTHEs using statistical methods, finding that louvered and vortex generator-modified designs outperform plain and wavy types in NPEI, despite increased pressure drop. Li et al. (2024) [26] optimized sinusoidal wavy fin-and-tube heat exchangers using CFD, achieving a 79.2% performance boost with a 23% rise in j-factor and 67.7% drop in f-factor. Kim et al. (2024) [27]

experimentally evaluated a PVTC with longitudinal fins and rectangular turbulators, achieving 42.73% higher total energy output than a smooth air channel PVTC. Hassen and Hameed et al. (2022) [28] examined a double-pipe heat exchanger with a square-cut turbulator, achieving a 271.7% increase in Nusselt number and a 117.6% rise in heat transfer. The 0.25 cm turbulator fin width demonstrated optimal thermal performance with minimal pressure drop. Skullong et al. (2024) [29] studied heat transfer in a tube with louver-punched triangular baffles, finding that smaller louvers and angles enhanced turbulence, maximizing thermal performance. Bhuiyan et al. (2022) [30] improved EGR cooler performance using vortex generators, with the Gothic-type wing VG achieving 12% better cooling than discrete ribbed and perforated louvered strip VGs.

Zhang et al. (2023) [31] investigated LFHEs enhanced with rectangular wing vortex generators, achieving optimal performance at  $N=7$ ,  $\beta=45^\circ$ ,  $HVG=1.8$  mm,  $WVG=1$  mm. This configuration improved PEC by up to 13.85% compared to the baseline. Duarte et al. (2023) [32] numerically examined heat transfer enhancement in a solar air heater using louvered-winglet vortex generators. Rectangular winglets and higher louver parameters improved thermo-hydraulic efficiency, achieving a maximum thermal enhancement factor. Alshibil et al. (2023) [33] experimentally analysed a bi-fluid PV/T collector with louvered fins, achieving up to 89.1% thermal and 7.66% electrical efficiency. The design significantly reduced solar cell temperature, enhancing energy output for various applications. Oh and Kim (2021) [34] analysed CVGs in fin-tube heat exchangers, finding DWU ( $\alpha=105^\circ$ ,  $r/R=1.25$ ) and DWD ( $\alpha=30^\circ$ ,  $r/R=1.5$ ) improved heat transfer by 5.2% and 7.5% with minimal pressure loss. Erbay et al. (2015) [35] studied how fin row number influences air-side performance of multilouvered heat exchangers under transient and quasi-steady conditions. They found that double-row fins provide higher heat transfer but also increased friction, while the number of rows has minimal impact on thermal-hydraulic performance during transient operation.

Sen et al. (2024) [36] investigated perforated dimple/protrusion fins, achieving a 23.7% PEC improvement. Optimal performance was observed with a 3.4 mm hole diameter, windward-side offset, and aligned configurations. Alnakeeb et al. (2021) [37] numerically studied a fin and flat-tube heat exchanger, finding that a 0.33 aspect ratio lowered pressure drop by 57.3% and boosted heat transfer per unit fan power by 111.5%. Shaeri et al. (2021) [38] used Design Builder simulations to optimize external louver angles for office buildings in three Iranian climates, finding climate-dependent angles that reduce solar heat gain and energy use, especially on south facades.

The research journey of louvered fins showcases a transition from fundamental modelling to advanced, application-specific designs that enhance thermal performance and energy efficiency. Innovations in geometry, material use, and turbulence management have yielded significant improvements in heat transfer rates and reduced pressure drops. These advances support diverse applications from solar energy systems and vehicular cooling to building-integrated systems proving the adaptability and effectiveness of louvered fins. The reviewed literature indicates that only a limited number of studies have focused on enhancing the thermo-hydraulic performance of louvered fin heat exchangers through geometric parameter modifications. A notable research gap exists in exploring the impact of varying louver fin shapes using different cutting patterns and design alterations. To bridge this gap, this project introduces a novel set of louver fin shape modifications and conducts a comprehensive analysis of their effects. The study

specifically evaluates the air-side thermo-hydraulic performance of the modified louvered fin heat exchangers. Key performance indicators, such as the Colburn j-factor, the friction f-factor and JF factor, are used to assess the thermal and flow characteristics of the proposed designs.

## **2 CFD ANALYSIS**

The thermal-hydraulic performance of louvered finned-tube heat exchangers is analysed using CFD to investigate the effects of various geometric parameters, including extended fin angles (90°, 120°, and 150°), extended fin lengths with 10%, 20% of its total length of the louver length across a Reynolds number range of 125 to 945. Various louver geometries were tested to evaluate their influence on thermal hydraulic performance with the parameters namely heat transfer coefficient, Nusselt number, temperature distribution, velocity profiles, and pressure drop.

### **2.1 PHYSICAL MODAL**

The overall dimensions of the louver finned heat exchanger are 160 mm (Height) x 160 mm (Width) x 15 mm (Depth), with the CFD domain designed at 4.50 mm (Width) x 1.50 mm (Height) x 7.50 mm (Depth). The louvered fin, featuring angled slits that create turbulence, increases heat transfer by disrupting the thermal boundary layer. The staggered fin arrangement guides airflow in a zigzag path, enhancing thermal interaction. These fins are widely used in automotive radiators, air conditioning units, and compact heat exchangers for efficient thermal management. The geometry significantly impacts factors like pressure drop and heat transfer efficiency. The CFD computational unit is selected based on the heat exchanger's symmetry, with boundaries defined by the center surfaces of adjacent fins and tube side surfaces. The detailed geometry of modified louver finned heat exchanger is shown in Fig. 1.

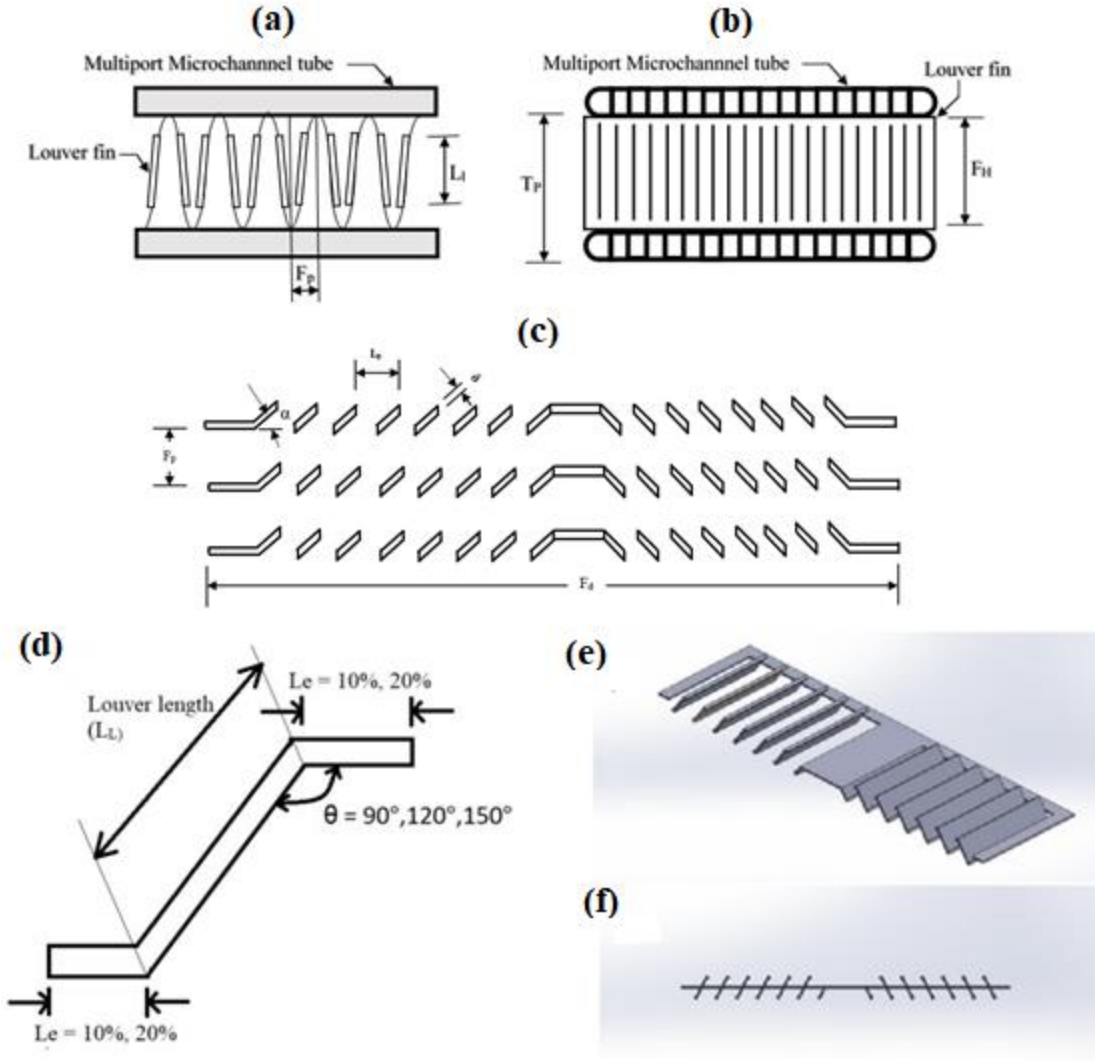


Fig. 1 Schematic diagram of modified louver fin arrangement (a) Front View, (b) Left side View, (c) Louver fin geometry (d) modified louver fin details (e) isometric view of the computational domain (f) front view of the computational domain

## 2.2 GOVERNING EQUATION

In this study, CFD simulations are conducted over a Reynolds number range (based on hydraulic diameter) from 400 to 4000, corresponding to louver pitch Reynolds numbers ( $Re_{lp}$ ) between 60 and 1800. Experimental findings confirm that the flow remains predominantly laminar up to  $Re_{lp} \approx 1300$ , despite minor unsteadiness near the louvers [10]. To analyse thermal and fluid behavior, the RNG  $k-\epsilon$  turbulence model is employed, revealing a 6–7% increase in heat transfer compared to laminar models. This minor variation justifies assuming laminar flow for  $Re_{lp} \leq 1300$ , while turbulent equations are applied for higher values. The simulations are governed by the conservation equations of mass, momentum, and energy.

Equations (1), (2), and (3) represent the governing equations applied to the three-dimensional simulation models.

$$\text{Mass,} \quad \nabla \cdot (\rho \cdot \vec{v}) = 0 \quad (1)$$

$$\text{Momentum,} \quad \nabla \cdot (\rho \cdot \vec{v})\vec{v} = -\nabla p + \nabla \cdot \left( \mu \left[ (\nabla \vec{v} + \nabla \vec{v}^T) - \frac{2}{3} \nabla \vec{v} I \right] \right) + \rho \vec{g} \quad (2)$$

Energy equation for steady state analysis is given in Eq. (3)

$$\nabla \cdot \left( \vec{v}(\rho E \cdot p) \right) = \nabla \cdot \left( k \cdot \nabla T - h\vec{j} + \left( \mu \left[ (\nabla \vec{v} + \nabla \vec{v}^T) - \frac{2}{3} \nabla \vec{v} I \right] \vec{v} \right) \right) \quad (3)$$

Where, Specific energy, E is defined by Eq. (4).

$$E = i - \frac{p}{\rho} + \frac{v^2}{2}$$

### 2.3 COMPUTATIONAL DOMAIN AND SOLUTION

The CFD analysis of the multilouvered fin heat exchanger was carried out using a three-dimensional computational domain that replicates a representative section of the fin geometry. This domain includes both the fluid and solid regions of the heat exchanger, comprising the air passage between the fins and the metal components responsible for conducting heat. The design ensures accurate representation of flow and thermal phenomena while maintaining computational efficiency by leveraging symmetry and periodicity. The detailed schematic diagram is illustrated in Fig. 2.

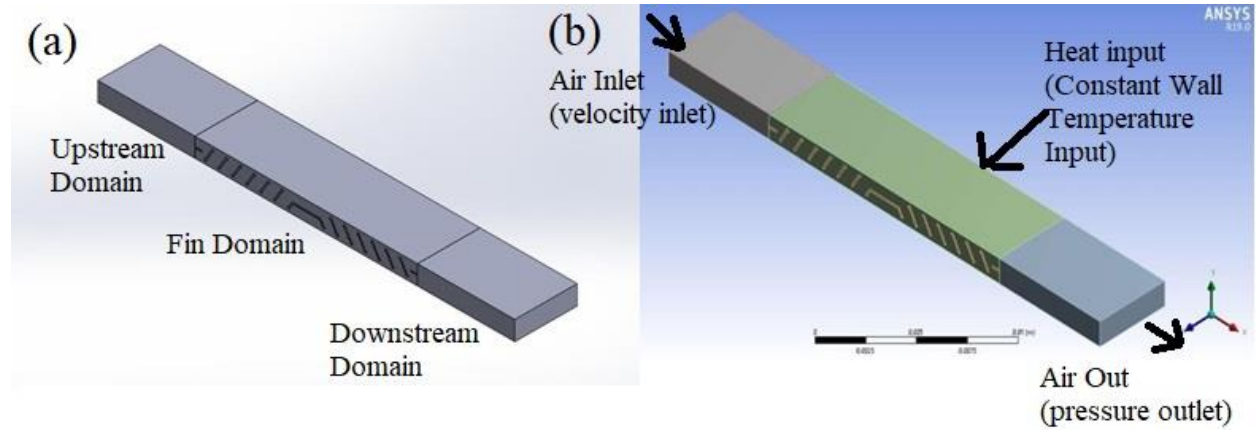


Fig. 2 Computation Domain and Boundary conditions

Boundary Conditions and assumptions are given as follows,

At the inlet, a uniform velocity profile is assumed, with the fluid entering the domain at a specified velocity  $u_{in}$ , and with no velocity components in the transverse or vertical directions:

$$u = u_{in}; \quad v = w = 0; \quad T = T_{in}$$

At the outlet, a pressure outlet boundary condition is imposed with a static gauge pressure and temperature specified. This ensures that the fluid exits the domain freely without reflecting backflow. To approximate fully developed flow, zero-gradient (Neumann) conditions are applied for velocity and temperature:

$$\frac{\partial u}{\partial x} = \frac{\partial v}{\partial x} = \frac{\partial z}{\partial x} = \frac{\partial T}{\partial x} = 0$$

The tube and fin walls are treated as no-slip adiabatic surfaces, except for the tube wall, which is maintained at a constant temperature of 323 K. This provides a thermal driving force for heat transfer from the wall to the fluid:

$$u = v = w = 0; \quad T = T_w = 323 \text{ K};$$

The top and bottom surfaces of the fluid domain are modelled using periodic boundary conditions, which reflect the repetitive nature of the louver fin array:

$$\frac{\partial u}{\partial z} = \frac{\partial v}{\partial z} = 0; \quad w = 0; \quad \frac{\partial T}{\partial z} = 0;$$

At the fluid-solid interface, continuity of temperature and heat flux is maintained. This ensures a physically accurate transition between conduction in the solid fin and convection in the fluid domain:

$$\frac{\partial u}{\partial y} = \frac{\partial w}{\partial y} = 0; \quad v = 0; \quad \frac{\partial T}{\partial y} = 0;$$

At the fluid-solid interface, continuity of temperature and heat flux is maintained. This ensures a physically accurate transition between conduction in the solid fin and convection in the fluid domain:

$$u = v = w = 0; \quad T_s = T_f; \quad k_{sl} \frac{\partial T_s}{\partial n} = k_{fl} \frac{\partial T_f}{\partial n};$$

For turbulent flow, turbulent intensity is defined as per correlation suggested in Fluent User's manual  $I = 0.16Re_d^{-1/8}$ . The finite volume method is employed to solve the continuity, momentum, and energy equations. Pressure-velocity coupling is handled using the SIMPLE algorithm. Spatial gradients are calculated with a least squares cell-based technique, while the momentum, energy, and pressure equations are discretized using a second-order upwind scheme. Relaxation factors are set at 0.3 for pressure, 0.7 for momentum, and 1 for energy. Convergence is achieved when residuals drop below  $10^{-5}$  for continuity and momentum, and  $10^{-7}$  for energy. The fin region is meshed with tetrahedral elements using proximity and curvature controls, while the upstream and downstream regions use hexahedral elements generated by an adaptive sizing function. To accurately capture boundary layer effects, inflation layers are applied on fin surfaces. Symmetry and periodic boundary conditions are used to model half the fin height, with uniform velocity and temperature specified at the inlet, and pressure boundary conditions at the outlet. No-slip conditions are applied on all solid surfaces. The grid creation of the modified louver fin is shown in Fig. 3.

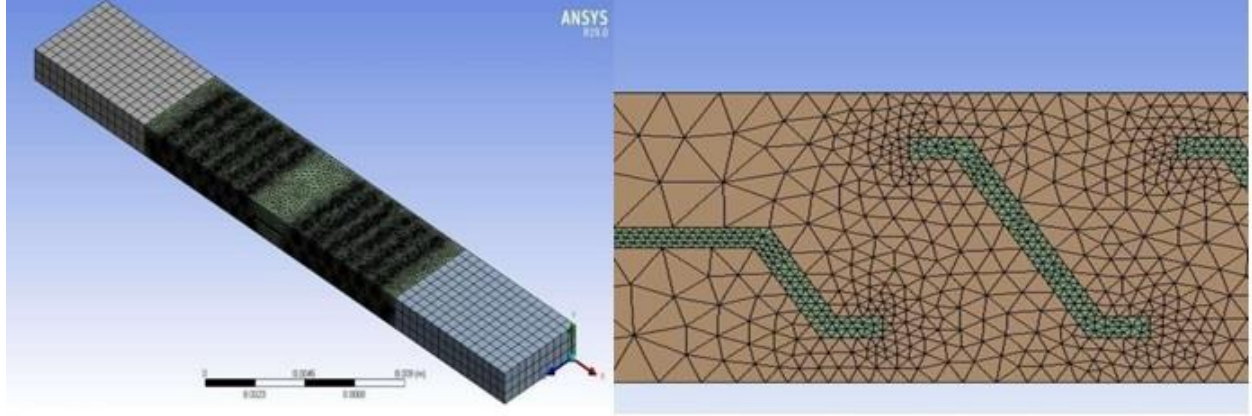


Fig. 3 Grid generation of the modified louver fin geometry

## 2.4 PERFORMANCE PARAMETERS

The performance of a multilouvered fin heat exchanger is significantly influenced by its flow behavior and geometric configuration, especially in compact systems where space and thermal efficiency are critical. This study evaluates both thermal and hydraulic characteristics using dimensionless and empirical parameters that quantify heat transfer effectiveness and flow resistance. The Reynolds number, which characterizes the flow regime, is defined based on the hydraulic diameter and louver pitch:

$$Re_d = \frac{\rho U D_h}{\mu} \quad (4)$$

$$Re_{Lp} = \frac{\rho U L_p}{\mu} \quad (5)$$

Where:  $\rho$  = density of air ( $\text{kg/m}^3$ ),  $\mu$  = dynamic viscosity ( $\text{Pa}\cdot\text{s}$ ),  $U$  = mean velocity ( $\text{m/s}$ ),  $D_h$  = hydraulic diameter ( $\text{m}$ ),  $L_p$  = louver pitch ( $\text{m}$ )

The hydraulic diameter is evaluated using the minimum flow area and wetted perimeter. The domain is split along the z-direction to calculate the upper domain's hydraulic diameter as:

$$D_H = 2D_{H,upper} \quad (6)$$

$$D_{H,upper} = 4(V_{supper}/S_{supper}) \quad (7)$$

To assess heat transfer performance, a conjugate heat transfer simulation is performed, assuming the fin walls and tubes are at a constant temperature of 323 K with infinite conduction. The air-side heat transfer coefficient is calculated using the log mean temperature difference (LMTD) method:

$$h = \frac{Q}{A \cdot LMTD} \quad (8)$$

$$LMTD = \frac{T_{a,out} - T_{a,in}}{\ln\left(\frac{T_W - T_{a,in}}{T_W - T_{a,out}}\right)} \quad (9)$$

To avoid overestimation caused by CFD sampling at wall-adjacent nodes, bulk temperatures are gathered from nodes away from the wall. The fin wall temperature and local heat transfer coefficient are computed as:

$$T_{fin\ wall} = \frac{q_w}{h_{wall}} + T_{wall\ adj.} \quad (10)$$

$$h_{local} = \frac{q_w}{T_{fin\ wall} - T_{bulk}} \quad (11)$$

$$St = \frac{h}{\rho U C_p} \quad (12)$$

For performance benchmarking, the Colburn j-factor and friction factor f are calculated as:

$$j = \frac{h}{\rho V_c C_p} Pr^{2/3} \quad (13)$$

$$f = \frac{2 \Delta p}{\rho V_c^2} * \frac{D_H}{L} \quad (14)$$

These parameters form the basis for evaluating the heat exchanger's overall performance. A higher j/f ratio indicates a favourable trade-off between heat transfer enhancement and pressure loss. This comprehensive evaluation of heat transfer coefficients, Nusselt number, pressure drop, and performance ratios provides a reliable framework for optimizing multilouvered fin geometries in compact heat exchangers.

## 2.5 GRID INDEPENDENT ANALYSIS

To ensure grid independence and accurate resolution of flow characteristics, both the upstream and downstream fluid domains were assigned a uniform hexahedral mesh size of 0.2 mm. The fin region, being more geometrically complex, was discretized using five different tetrahedral mesh densities, with element sizes of 0.25 mm, 0.2 mm, 0.1 mm, 0.08 mm, and 0.045 mm. The schematic diagram of computation domain and grid independence test is illustrated in Fig. 4. These mesh configurations corresponded to total element counts of approximately 4951256, 3989869, 3125458, 1985063 and 495488 respectively. The air-side heat transfer coefficient was used as the performance parameter to evaluate mesh sensitivity. The heat transfer coefficient and pressure drop values showed significant fluctuations during the initial stages of mesh refinement, indicating sensitivity to grid resolution. However, as the mesh density increased, these parameters gradually converged, and beyond approximately 3125458 elements the changes became minimal, demonstrating that further refinement provided no meaningful improvement in solution accuracy. Based on this observed convergence behaviour, a mesh corresponding to nearly 3125458 elements was selected for all subsequent simulations, as it offered an optimal balance between computational efficiency and numerical precision while ensuring reliable and grid-independent results.

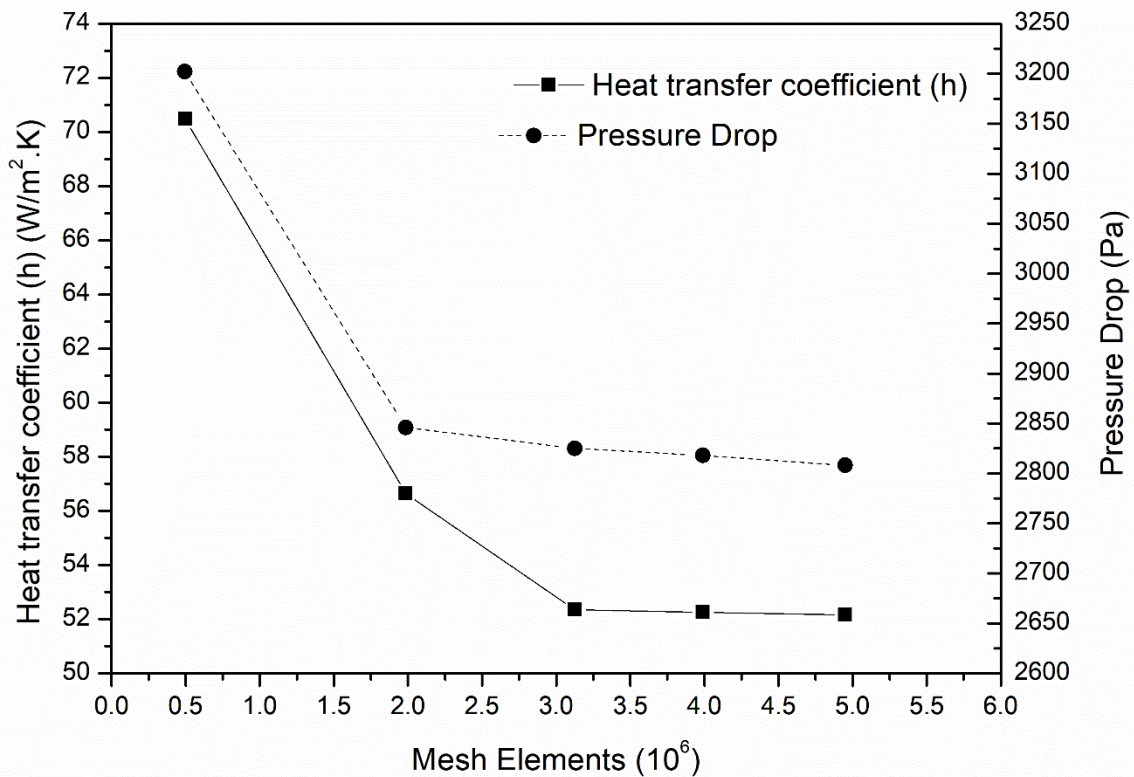


Fig. 4 Grid independence test

## 2.6 VALIDATION STUDY

The numerical analysis of the air-side thermal-hydraulic performance was conducted for Reynolds numbers ranging from 125 to 945. The model included conjugate heat transfer and fin thermal resistance to closely replicate real conditions. For validation, two specific configurations from Malapure et al. (2007) [17] numerical data were selected: Configuration 1 with a louver pitch of 1.4 mm, louver angle of 25.5°, fin pitch of 2.02 mm, hydraulic diameter of 3.33 mm; and Configuration 9 with a louver pitch of 0.81 mm, louver angle of 29°, fin pitch of 1.72 mm and hydraulic diameter of 2.86 mm. The computational domain modelled half the fin height using symmetry boundary conditions. The comparison of Stanton number and friction factor between present study and Malapure et al (2007) [17] data showed strong agreement at all the Reynolds numbers and it has the difference between in the range of 10-12% for Stanton number and 8-11% for f factor respectively. This is shown in Fig. 5.

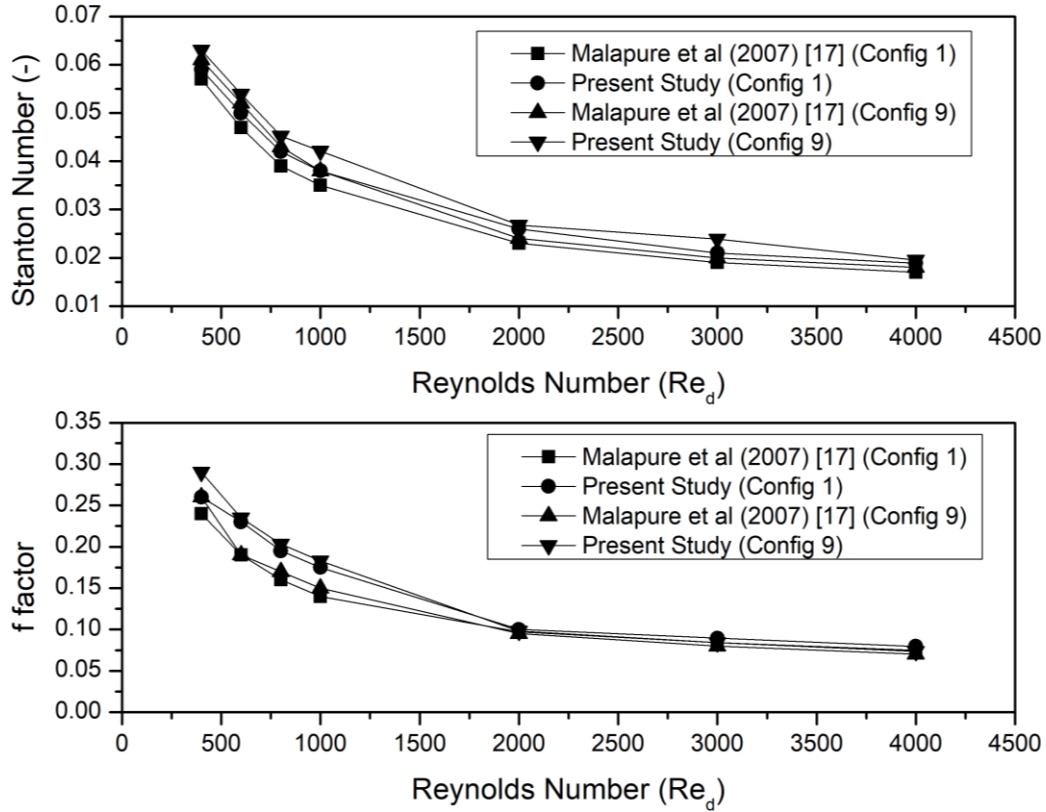


Fig. 5 Validation Study

### 3 RESULTS AND DISCUSSION

The performance of the louvered fin heat exchanger was evaluated based on five key parameters: heat transfer coefficient, Nusselt number, pressure drop, j-factor, and f-factor.

#### 3.1 Heat Transfer Coefficient

Fig. 6 illustrated the contour plot of temperature distribution in modified louver fin geometry at  $Re_{lp} \approx 745$ . It confirms that the temperature distribution is more in  $120^\circ$ -20 louver fin geometry compared to all other fin geometries. Fig 7 shows that velocity distribution for modified louver fin geometry for  $90^\circ$ ,  $120^\circ$  and  $150^\circ$ . The louver-fin geometry consists of periodically inclined fin segments that redirect the incoming airflow, generating strong recirculation zones and vortex structures downstream of each louver, as evidenced by the velocity contours and streamlines, which enhance mixing and promote boundary-layer disruption for improved convective heat transfer. Due to extension of the louver fin, recirculation flow has been occurred in between the louver fins. This will enhance heat transfer and pressure drop characteristics. Fig. 8 illustrates the heat transfer coefficient variation with various louver angle for different pitches. The heat transfer coefficient increases steadily with Reynolds number across all configurations, showing enhanced convective activity at higher flow rates. Among all, the  $120^\circ - 20\%$  setup achieves the highest value, peaking near  $64 \text{ W/m}^2\cdot\text{K}$  at  $Re_{lp} \approx 945$ , due to optimal boundary layer disruption. Comparing  $90^\circ$  and  $150^\circ$  angles, intermediate  $120^\circ$  consistently outperforms both, indicating a superior louver alignment for thermal enhancement. Additionally, across all angles, 20% pitch ratio yields better performance than

10%, affirming the influence of pitch optimization on flow reattachment and surface exposure. Among all, the 120° – 20% setup achieves the highest value, peaking near 64 W/m<sup>2</sup>·K at Re<sub>lp</sub> ≈ 945, due to optimal boundary layer disruption. Comparing 90° and 150° angles, intermediate 120° consistently outperforms both, indicating a superior louver alignment for thermal enhancement. Additionally, across all angles, 20% pitch ratio yields better performance than 10%, affirming the influence of pitch optimization on flow reattachment and surface exposure. The rapid rise in thermal performance between Re = 150-330 is due to the advent of increased flow mixing and improved louver-directed flow realignment, which becomes increasingly effective when inertial forces begin to dominate viscous forces in this Reynolds number range. At low Reynolds numbers, the flow is weak and partially attached, so even a small increase in Re significantly increases cross-flow penetration through the louvers, promoting flow reorientation, earlier boundary-layer disruption, and improved convective transport—resulting in a dramatic increase in the heat transfer coefficient.

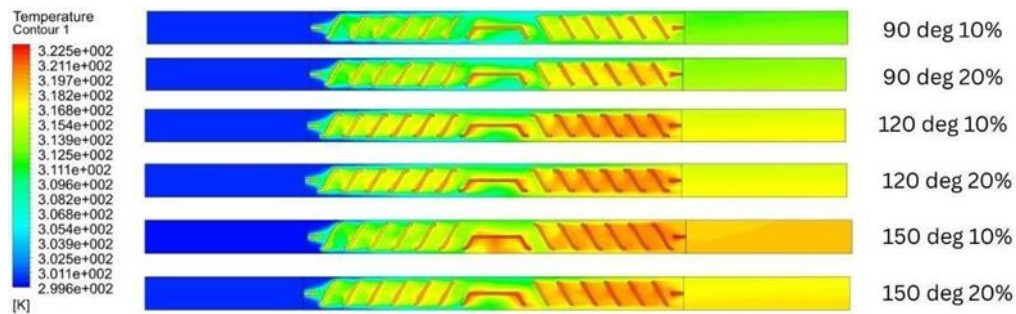


Fig. 6 Contour plot for temperature distribution in modified louver fin geometry

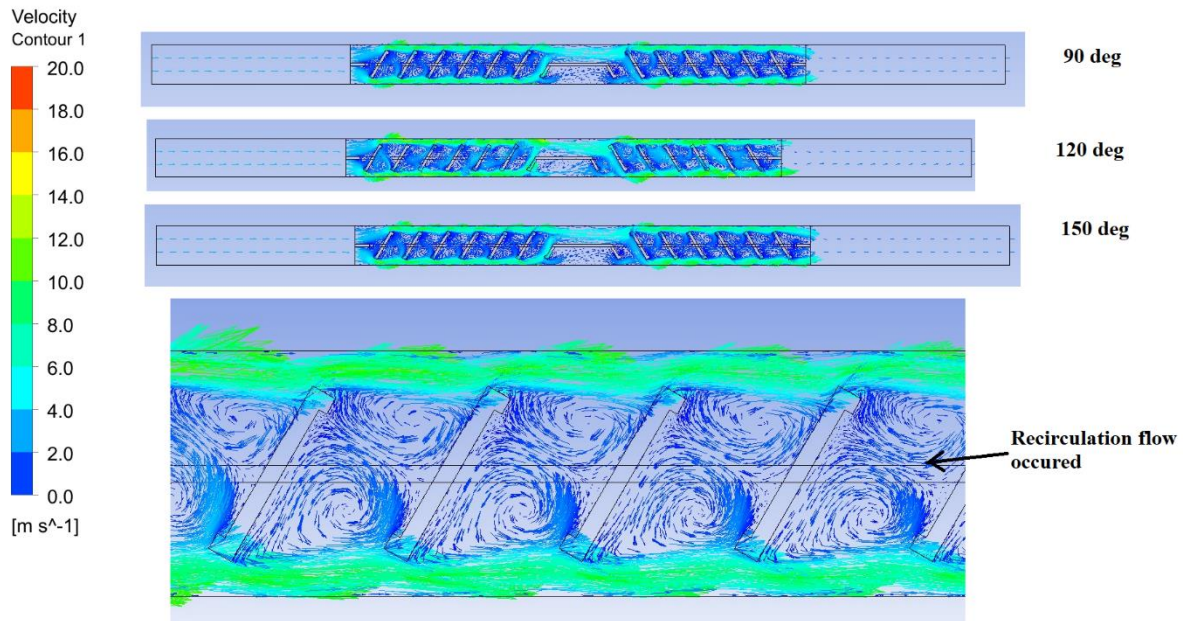


Fig 7. Vector plot for velocity fields for modified louver fin geometry

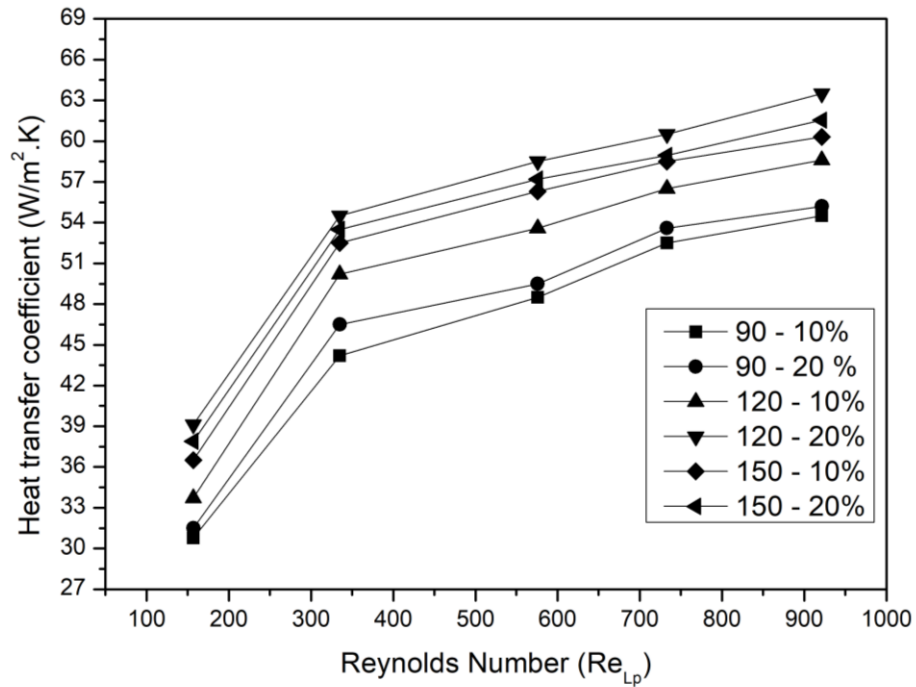


Fig.8 Variation of heat transfer coefficient for several louver angle with various pitches

### 3.2 Nusselt Number

The Nusselt number trends upward with Reynolds number for all configurations, but the rate of increase slows beyond  $Re_{ip} = 600$ , indicating diminishing returns in convective enhancement and it is shown in Fig. 9. At higher flow rates,  $120^\circ - 20\%$  consistently exhibits superior performance, with a peak Nusselt number above 40, reflecting effective turbulence generation and surface utilization. Unlike the pressure drop curve, where  $150^\circ$  underperformed, here it holds middle ground—confirming that thermal and hydraulic behaviors are not always directly correlated. Pitch ratio again plays a noticeable role, with 20% outperforming 10%, particularly at mid to high Reynolds numbers.

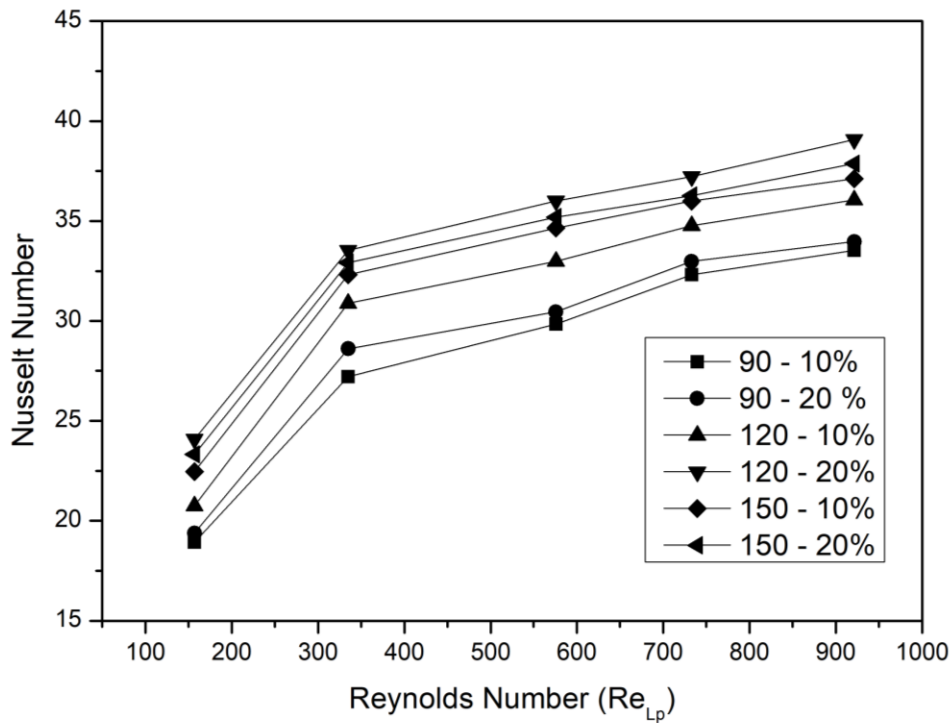


Fig. 9 Variation of Nusselt number for different Reynolds number

### 3.3 Pressure Drop

Fig. 10 illustrates the contour plot for pressure drop for different louver angles. It shows that pressure drop does not majorly varied. Variation of pressure drop characteristics for several louver angles at different Reynolds number are illustrated in Fig. 11. Pressure drop increases linearly with Reynolds number across all configurations, highlighting higher flow resistance at increased velocities. Notably, the  $150^\circ - 10\%$  and  $150^\circ - 20\%$  configurations produce the highest-pressure drops, nearing 740 Pa at  $Re_{lp} \approx 945$ , indicating more flow obstruction due to sharper fin angles and tighter spacing. Unlike the thermal performance where  $120^\circ$  dominated, here wider angles like  $150^\circ$  create excessive drag, showing the trade-off between heat transfer gain and pressure penalty. The difference between 10% and 20% pitch ratios is relatively minor in pressure performance, suggesting geometry has a stronger influence than pitch here.

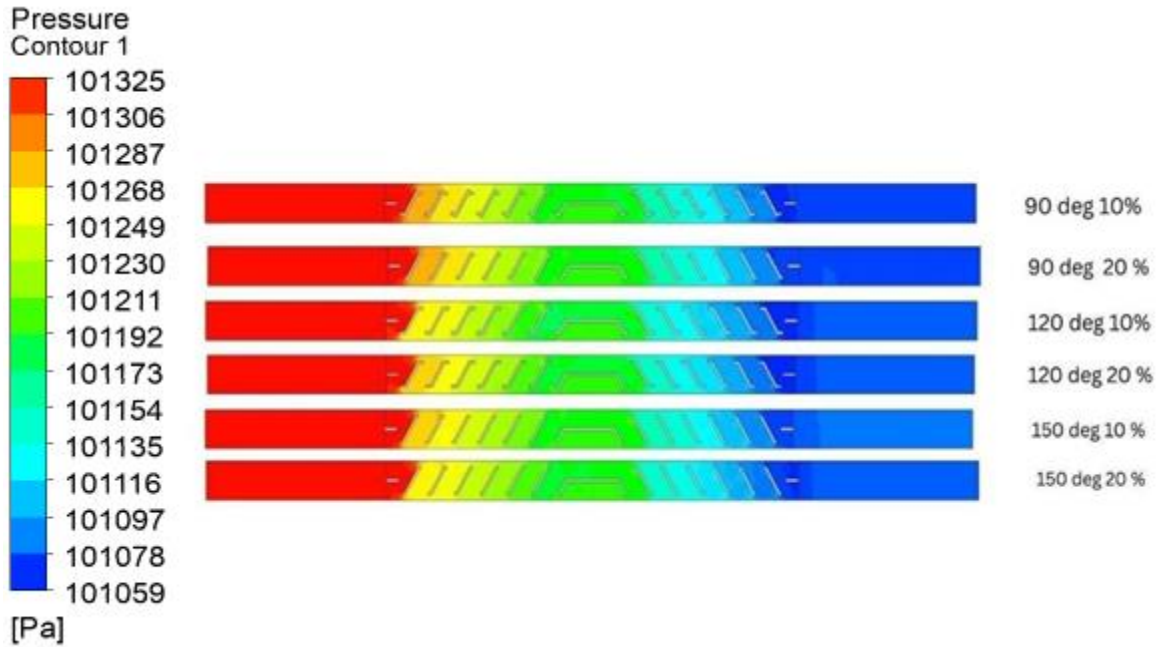


Fig. 10 contour plot for pressure drop for different louver angle with various pitch values at  $Re_{ip} = 945$ .

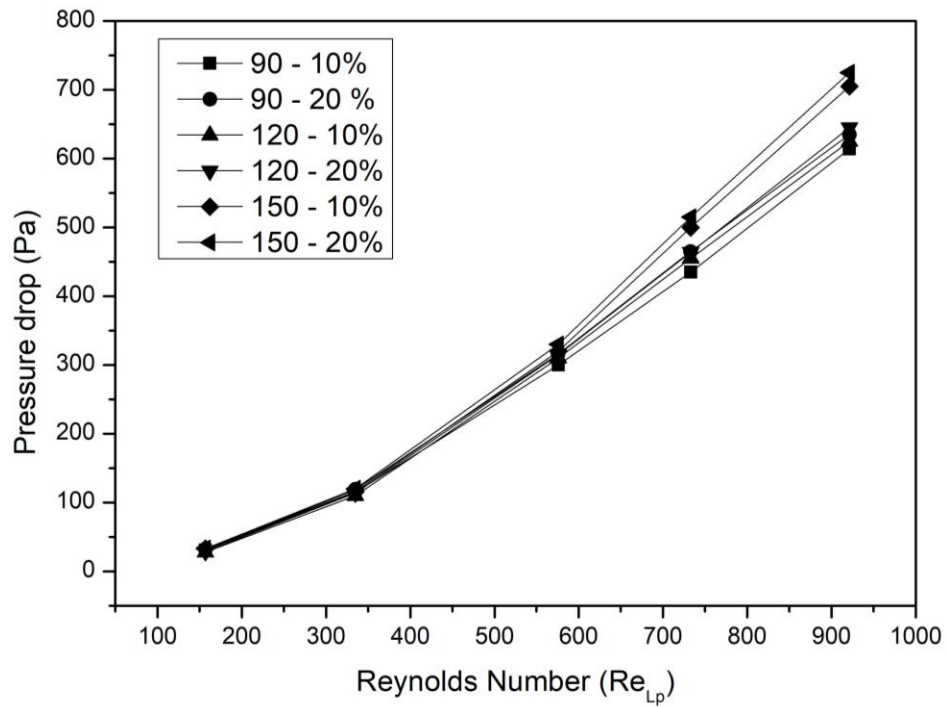


Fig. 11 Variation of Pressure drop for various Reynolds numbers

### 3.4 j and f Factor

Fig. 12 illustrates the variation of j factor and f factor for different Reynolds number. As Reynolds number increases, the j-factor (left axis) declines steadily across all configurations, reflecting reduced convective enhancement per unit velocity. In contrast, the f-factor (right axis) also drops, but more gradually—indicating a proportional decline in flow resistance. Interestingly, 90° – 20% and 120° – 20% yield the highest j-values at lower Reynolds numbers, while 150° – 10% shows relatively elevated f-values throughout. This suggests that more aggressive louver geometries can maintain thermal advantage in the low-to-mid Re range but begin losing efficiency as flow transitions toward turbulence. The divergence in j and f behavior underscores the importance of considering both simultaneously for optimal design.

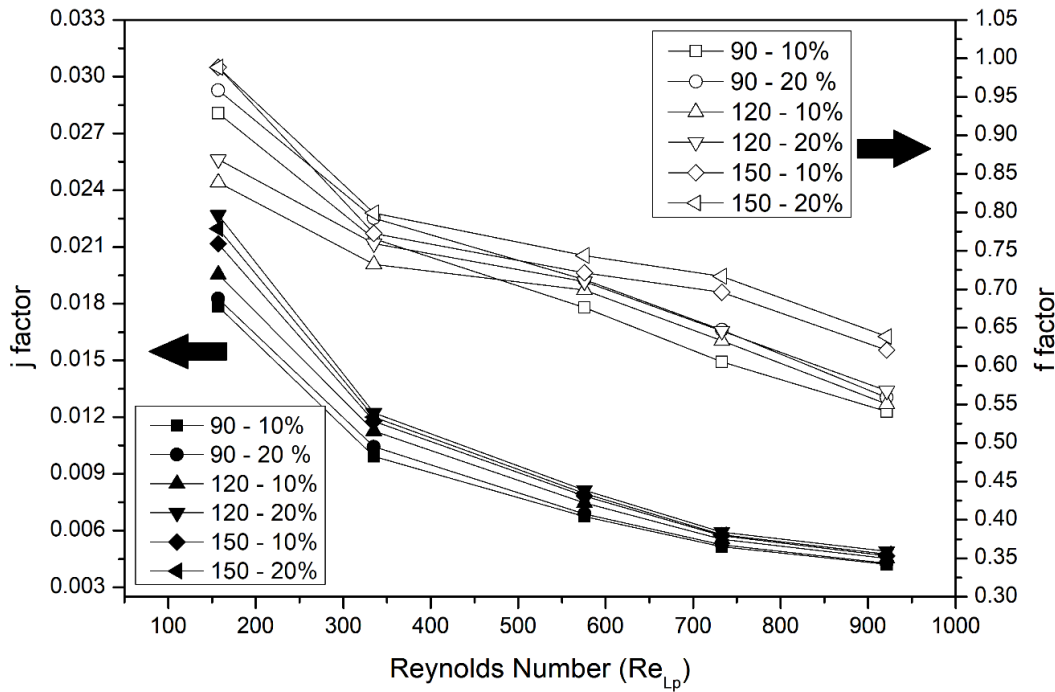


Fig. 12 Variation of j and f factor for different louver angles at different Reynolds numbers

### 3.5 JF Factor

The JF factor, which reflects the thermal-hydraulic performance trade-off, decreases sharply with increasing Reynolds number across all configurations and it is illustrated in Fig. 13. While this trend is expected due to the rising dominance of inertia over heat transfer gains at higher flow rates, the 120° – 20% and 120° – 10% geometries maintain relatively better values throughout. Unlike earlier plots, here the focus shifts to the rate of decay, where steeper drops at lower Re suggest rapidly diminishing relative efficiency. The close clustering of lines beyond  $Re_{ip} = 600$  also suggests limited advantage in pushing the flow further in terms of j/f performance.

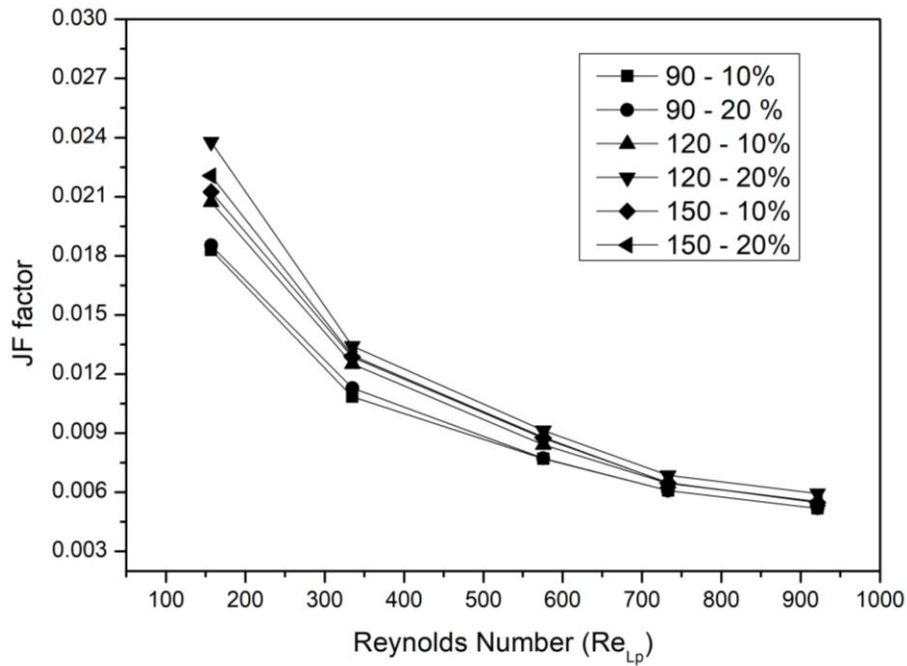


Fig. 13 Variation of JF factor for different Reynolds numbers

#### 4 CONCLUSIONS

The CFD analysis reveals that fin geometry and pitch ratio critically influence the thermal and hydraulic performance of multilouvered heat exchangers.

- Comparing 90° and 150° angles, intermediate 120° consistently outperforms both, indicating a superior louver alignment for thermal enhancement. Additionally, across all angles, 20% pitch ratio yields better performance than 10%, affirming the influence of pitch optimization on flow reattachment and surface exposure.
- At higher flow rates, 120° – 20% consistently exhibits superior performance, with a peak Nusselt number above 40, reflecting effective turbulence generation and surface utilization.
- Pressure drop penalties were more severe with wider angles like 150°, emphasizing a performance trade-off. Unlike the thermal performance where 120° dominated, here wider angles like 150° create excessive drag, showing the trade-off between heat transfer gain and pressure penalty.
- The  $j$  and  $f$  factors exhibited distinct decline rates, highlighting the nuanced interplay between convection and resistance.
- The JF factor trends confirmed that optimal efficiency lies in moderate  $Re$  ranges with well-tuned geometry.
- Overall, the 120°–20% setup emerges as the most promising for compact, high-performance cooling applications.
- It was observed that optimized geometric configurations (the 120° louver angle with 20% pitch) led to a significant enhancement in heat transfer characteristics (high  $h$ ,  $Nu$ , and  $j$ ) while

maintaining a relatively low pressure drop and friction factor ( $\Delta P$  and  $f$ ). These trends clearly indicate a favourable thermal-hydraulic performance.

- The results also validated the effectiveness of the selected louver geometry and mesh strategy in capturing realistic flow and heat transfer behavior.

### Declaration of Competing Interest

The authors state that they have no financial or personal connections that could have influenced the work in this paper.

### Nomenclature

1. CFD - Computational Fluid Dynamics (-)
2.  $h$  – heat transfer coefficient ( $W/m^2.K$ )
3.  $Nu$  – Nusselt number (-)
4.  $j$  – Colburn j-factor (-)
5.  $f$  – friction factor (-)
6.  $\Delta P$  - Pressure Drop (Pa)
7.  $Re$  – Reynolds number (-)
8.  $Le$  - extender fin length (mm)
9.  $Re_{ip}$  - Reynolds number based on louver pitch (-)
10.  $u_{in}$  – air velocity inlet (m/s)
11. LMTD - Log Mean Temperature Difference (-)
12.  $T_w$  - Wall temperature (K)
13.  $St$  – Stanton Number (-)
14.  $Pr$  – Prandtl Number (-)

### References

- [1] Kays, W.M. and London, A.L., *Compact heat exchangers*, (1984).
- [2] Shah, R.K., Sekulić, D.P., *Fundamentals of Heat Exchanger Design*, John Wiley & Sons, Hoboken, NJ, USA, 2003.
- [3] Shah, R. K., *Comprehensive Study of Heat Exchangers with Louvered Fins in Heat Exchangers – Advanced Features and Applications*, Springer, New York, 2020.
- [4] Chand, S. and Chand, P., Parametric study on the performance of solar air heater equipped with louvered fins. *Journal of Mechanical Science and Technology*, 32 (2018), pp.3965-3973. <https://doi.org/10.1007/s12206-018-0747-y>
- [5] Sønderby., *et al.*, Thermal-hydraulic performance of a corrugated cooling fin with louvered surfaces. *Energy Procedia*, 142 (2017) pp. 4077-4084. <https://doi.org/10.1016/j.egypro.2017.12.328>
- [6] Lin, C.W. and Jang, J.Y., 3D Numerical heat transfer and fluid flow analysis in plate-fin and tube heat exchangers with electrohydrodynamic enhancement. *Heat and mass transfer*, 41(7) (2005), pp.583-593. <https://doi.org/10.1007/s00231-004-0540-6>
- [7] Moosavi, R., *et al.*, Investigation of the geometrical structure of louvered fins in fin-tube heat exchangers for determining the minimum distance of the headers. *Journal of Mechanical Science and Technology*, 35(2021), pp.1721-1731. <https://doi.org/10.1007/s12206-021-0335-4>

- [8] Kim, Nae-Hyun. Air-side heat transfer and pressure drop of the fin-and-tube heat exchangers having oval tubes under wet condition. *Heat and Mass Transfer*, 57, no. 10 (2021), pp.1633-1644. <https://doi.org/10.1007/s00231-021-03058-1>
- [9] Kannadhasan, V., *et al.*, Experimental research and CFD analysis on engine fins with varied geometries. *Interactions*, 245, no. 1 (2024): 260. <https://doi.org/10.1007/s10751-024-02101-x>
- [10] Achaichia, A and Cowell, T.A, Heat transfer and pressure drop characteristics of flat tube and louvered plate fin surfaces, *International Journal of Heat and Mass Transfer*, 31 (1988), pp. 119-128.
- [11] Kim, M.H. and Bullard, C.W., Air-side thermal hydraulic performance of multi-louvered fin aluminum heat exchangers. *International journal of refrigeration*, 25(3) (2002), pp.390-400.
- [12] Wongwises, Somchai, and Yutasak Chokeman. Effect of fin thickness on air-side performance of herringbone wavy fin-and-tube heat exchangers. *Heat and mass transfer*; 41 (2004) pp. 147-154. <https://doi.org/10.1007/s00231-004-0507-7>
- [13] Li, Yong, *et al.*, Effect of shape and placement of twisted pin fins in a rectangular channel on thermo-hydraulic performance. *Journal of Thermal Science*, 33, no. 5 (2024), pp. 1773-1793. <https://doi.org/10.1007/s11630-024-2030-0>
- [14] Zhu, Yuxi, and Yan Qiu. Comparison of thermal performance between annular fins and longitudinal fins in latent heat storage unit. *Journal of Thermal Science*, 32, no. 3 (2023), pp. 1227-1238. <https://doi.org/10.1007/s11630-023-1731-0>
- [15] Mozafarie, Seyed Shahab, and Kouros Javaherdeh. "Numerical design and heat transfer analysis of a non-Newtonian fluid flow for annulus with helical fins. *Engineering Science and Technology, an International Journal*, 22, no. 4 (2019), pp. 1107-1115. <https://doi.org/10.1016/j.jestch.2019.03.001>
- [16] Lindqvist, Karl, *et al.*, "Plate fin-and-tube heat exchanger computational fluid dynamics model. *Applied Thermal Engineering*, 189 (2021), pp. 116669. <https://doi.org/10.1016/j.applthermaleng.2021.116669>
- [17] Mercan, Hatice, *et al.*, Determination of heat transfer rates of heavy-duty radiators for trucks having flattened and double-U grooved pipes with louvered fins by ANN method: an experimental study. *The European Physical Journal Plus*, 137, no. 3 (2022), pp. 382.
- [18] Santosa, IDewa MC, *et al.*, Experimental and CFD investigation of overall heat transfer coefficient of finned tube CO<sub>2</sub> gas coolers. *Energy Procedia*, 161 (2019), pp. 300-308. <https://doi.org/10.1016/j.egypro.2019.02.096>
- [19] Li, Jun, *et al.*, Effect of flow maldistribution on heat transfer performance and temperature field of plate-fin heat exchangers. *International Communications in Heat and Mass Transfer*, 149 (2023) pp. 107135. <https://doi.org/10.1016/j.icheatmasstransfer.2023.107135>
- [20] Arunkumar, H. S., *et al.*, Energy exergy and economic analysis of a multiple inlet solar air heater for augmented thermohydraulic performance. *Applied Thermal Engineering*, 246 (2024), pp. 122981. <https://doi.org/10.1016/j.applthermaleng.2024.122981>

- [21] Kumar, S. *et al.*, Optimization of louver fin geometries for miniature microchannel condenser by Taguchi and CFD method. *Sādhanā*, 49, no. 3 (2024) pp. 216. <https://doi.org/10.1007/s12046-024-02558-0>
- [22] Malapure, V. *et al.*, Numerical investigation of fluid flow and heat transfer over louvered fins in compact heat exchanger. *International journal of thermal sciences*, 46, no. 2 (2007), pp. 199-211. <https://doi.org/10.1016/j.ijthermalsci.2006.04.010>
- [23] Erbay, L. Berrin, *et al.* Numerical investigation of the air-side thermal hydraulic performance of a louvered-fin and flat-tube heat exchanger at low Reynolds numbers, *Heat Transfer Engineering*, 38.6, (2017), pp. 627-640.
- [24] Feleke, Dessalew Shite *et al.*, Numerical investigation of louver edges effect on the performances of louvered fin compact heat exchanger. *Heliyon*, 10, no. 6 (2024). <https://doi.org/10.1016/j.heliyon.2024.e27254>
- [25] Reshaeel, Muhammad, *et al.*, A critical review of the thermal-hydraulic performance of fin and tube heat exchangers using statistical analysis. *International Journal of Thermofluids*, 24 (2024): 100858. <https://doi.org/10.1016/j.ijft.2024.100858>
- [26] Li, Yang, *et al.*, Multi-objective shape characterization of airside performance in sinusoidal wavy fin-and-tube heat exchangers with large-diameter tubes using CFD. *Journal of Mechanical Science and Technology*, 38, no. 7 (2024), pp. 3837-3848. <https://doi.org/10.1007/s12206-024-0652-5>
- [27] Kim, Seong-Bhin, *et al.*, Experimental performance evaluation of air-based photovoltaic–thermal collector with rectangular turbulators and longitudinal fins. *Energy Reports*, 12 (2024), pp. 1315-1324. <https://doi.org/10.1016/j.egy.2024.07.038>
- [28] Hassan, Jannah Haitham, and Vinous M. Hameed. "Evaluate the hydrothermal behavior in the heat exchanger equipped with an innovative turbulator. *South African Journal of Chemical Engineering*, 41 (2022), pp. 182-192. <https://doi.org/10.1016/j.sajce.2022.06.003>
- [29] Jayranaiwachira, Nuthvipa, *et al.*, Heat transfer analysis in a tube contained with louver-punched triangular baffles. *Results in Engineering*, 22 (2024), pp. 102276. <https://doi.org/10.1016/j.rineng.2024.102276>
- [30] Hasan, Md Jahid, *et al.*, Improvement of an exhaust gas recirculation cooler using discrete ribbed and perforated louvered strip vortex generator. *International Journal of Thermofluids*, 13 (2022), pp. 100132. <https://doi.org/10.1016/j.ijft.2022.100132>
- [31] Zhang, Jinglong, *et al.*, Effects of rectangular wing vortex generators on the thermal-hydraulic performance of louvered fin and flat tube heat exchanger. *Journal of Thermal Science*, 32, no. 2 (2023), pp. 628-642. <https://doi.org/10.1007/s11630-023-1763-5>
- [32] Duarte, Rafael MD, *et al.*, Numerical investigation of heat transfer enhancement by using louvered-winglet vortex generators mounted in a solar air heater channel-type. *Journal of Thermal Analysis and Calorimetry*, 148, no. 24 (2023), pp. 14183-14204. <https://doi.org/10.1007/s10973-023-12599-y>
- [33] Alshibil, Ahssan MA, *et al.*, Experimental performance comparison of a novel design of bi-fluid photovoltaic-thermal module using Louver fins. *Energy Reports*, 9 (2023), pp. 4518-4531. <https://doi.org/10.1016/j.egy.2023.03.110>

- [34] Ali, Samer, *et al.*, Advancing thermal performance through vortex generators morphing. *Scientific Reports*, 13, no. 1 (2023), pp. 368. <https://doi.org/10.1038/s41598-022-25516-4>
- [35] Dogan, Bahadır, *et al.*, An experimental comparison of two multi-louvered fin heat exchangers with different numbers of fin rows, *Applied Thermal Engineering*, 91 (2015), pp. 270-278.
- [36] Sen, Palash, *et al.*, Heat transfer enhancement of air flow through new types of perforated dimple/protrusion fins. *Applied Thermal Engineering*, 256 (2024), pp. 124030. <https://doi.org/10.1016/j.applthermaleng.2024.124030>
- [37] Alnakeeb, Mohamed A., *et al.*, Numerical investigation of thermal and hydraulic performance of fin and flat tube heat exchanger with various aspect ratios. *Alexandria Engineering Journal* 60, no. 5 (2021), pp. 4255-4265. <https://doi.org/10.1016/j.aej.2021.03.036>
- [38] Shaeri, Jalil, *et al.*, Effects of External Louvers on Solar Heat Gain and Energy Consumption of an Office Building in Different Climates of Iran. *Iranian Journal of Science and Technology, Transactions of Mechanical Engineering*, (2022), pp. 1-16. <https://doi.org/10.1007/s40997-021-00449-x>

Received: 3.8.2025.

Revised: 25.11.2025.

Accepted: 5.12.2025.